AN INTRODUCTION TO PASSIVE MICROWAVE REMOTE SENSING AND ITS APPLICATIONS TO METEOROLOGICAL ANALYSIS AND FORECASTING

Ralph R. Ferraro

NOAA/NESDIS/Office of Research and Applications
Camp Springs, Maryland

Sheldon J. Kusselson

NOAA/NESDIS/Satellite Analysis Branch
Camp Springs, Maryland

Marie Colton

Office of Naval Research
Arlington, Virginia

Abstract

Passive microwave observations from the polar orbiting Defense Meteorological Satellite Program, Special Sensor Microwave Imager (SSM/I) are now widely used in an assortment of meteorological analysis and forecasting applications. Since most of the operational forecasting community is familiar with visible and infrared satellite imagery but not with those from the SSM/I, this paper first presents an introduction to basic principles of passive microwave remote sensing. A short review of the current satellite missions containing microwave radiometers is presented. The retrieval algorithms and applications for several products (e.g., total precipitable water, rain rate, ocean surface wind speed, snow cover and sea-ice cover) are described and examples of the products are illustrated. The paper also presents a list of Internet web sites where many of these products can be found.

1. Introduction

Most weather forecasters and satellite analysts are familiar with satellite measurements taken at visible (VIS) and infrared (IR) portions of the spectrum, and taken primarily from geosynchronous satellites (e.g., GOES series). Loops of GOES imagery have become the cornerstone of meteorological analysis and nowcasting. There is another type of operational satellite sensor, used routinely by defense and civilian agencies, that is valuable in aiding in the interpretation of meteorological surface observations and GOES satellite imagery. These measurements originate from passive microwave observations taken by the Special Sensor Microwave Imager (SSM/I), which is flown aboard the Defense Meteorological Satellite Program (DMSP) polar orbiting satellite series. This sensor can provide information under virtually all weather conditions. Since the SSM/I has seven independent measurements, simultaneous retrievals can be performed to obtain information on several meteorological parameters, including rain rate, water vapor, and snow cover. In addition, the retrievals are made using objective algorithms thereby requiring very little human intervention or the use of ancillary data.

The first SSM/I instrument was launched on 19 June 1987 aboard the DMSP F-8 satellite. Other instruments have successfully operated on board the F-10 (December 1990), F-11 (November 1991), F-13 (April 1995), and F-14 (September 1997) satellites, the latter two of which are currently operational. The SSM/I is a seven channel radiometer measuring earth emitted radiation at 19.35, 22.235, 37.0, and 85.5 GHz. All of the measurements are dual-polarization except at 22.235 GHz, where only vertical polarization is measured. The DMSP satellites operate in a sun-synchronous orbit[1] with an orbital period of about 102 minutes and have an orbital swath width of 1400 km. The characteristics of the SSM/I are summarized in Table 1 and Fig. 1. More detail about the SSM/I can be found in Hollinger (1991). Because the SSM/I operates in a 'conical scan' mode (e.g., fixed incidence angle with Earth's surface), it's swath width is relatively narrow and so adjacent orbits will have 'gaps' between them equatorward of about 50 degrees latitude. In addition to the polar temporal sampling limitation (e.g., twice a day), this spatial sampling pattern also contributes to the limitation in using the data for very short term synoptic/mesoscale forecasting applications. The problem is somewhat alleviated by the fact that there are two operational SSM/I sensors, which have overpass times that are about 4 hours apart (e.g., 0600 and 1000, and 1800 and 2200 LST).

There are two purposes of this paper. The first is to describe the physical basis of microwave radiative transfer and to introduce the SSM/I product suite to the operational weather forecaster. These are discussed in section 2. The second purpose is to provide detail on the retrieval algorithms and describe their use by operational agencies. This is provided in section 3. The paper concludes by

[1] Polar orbiting satellites are designed to be 'sun synchronous,' which means that they pass over a given location at the same local time each day. There are two passes a day, ascending and descending.

Table 1. SSM/I Sensor Characteristics.

SSM/I Channels	Frequency (Polarization)	Spatial Resolution	Possible Uses
1,2	19.35 GHz (V, H)	43 x 69 km	1. Sea-Ice Cover 2. Ocean Cloud Water and Rainfall 3. Land/Water Boundaries 4. Soil Moisture 5. Vegetative Cover/Roughness
3	22.235 GHz (V)	40 x 60 km	1. Oceanic Water Vapor
4,5	37.0 GHz (V, H)	29 x 37 km	1. Ocean Cloud Water and Rainfall 2. Ocean Surface Winds 3. Heavy Convective Rain Over Land 4. Snow Cover 5. Sea-Ice Cover
6,7	85.5 GHz (V, H)	13 x 15 km	1. Land/Ocean Rainfall 2. Non-raining Clouds Over Ocean 3. Snow Cover 4. Sea-Ice Cover

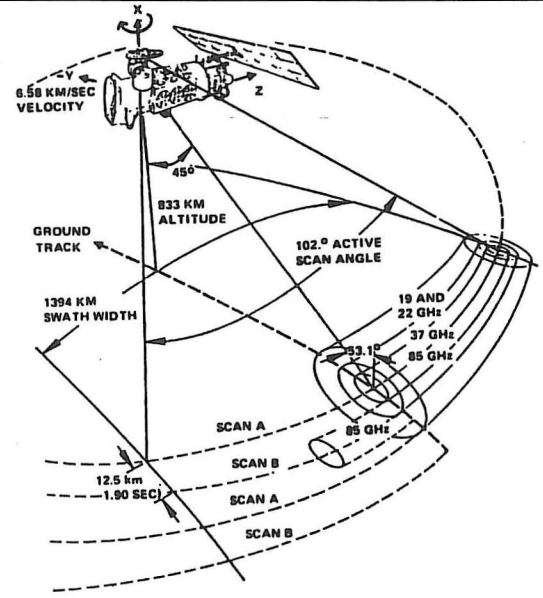

SCAN A	
SCENE STATIONS/SCAN	128
PIXELS/SCAN	576
SCAN B	
SCENE STATIONS/SCAN	128
PIXELS/SCAN	256
SCENE STATIONS/ORBIT	404,224
PIXELS/ORBIT	1,313,728

Fig. 1. SSM/I sensor scanning characteristics (after Hollinger 1991).

discussing the current and future status of operational passive microwave sensors. A list of acronyms is provided at the end of the paper to aid the reader and to serve as a future reference guide.

2. Background

a. Physical principles

Microwave (MW) energy is naturally emitted from the earth-atmosphere system. As is shown in Fig. 2, MW wavelengths are much longer than those at the VIS and IR portion of the spectrum. "Passive" microwave sensors, or radiometers, are designed to sense this energy. This is in contrast to "active" MW sensors such as weather radar, which measure the return signal from a pulse of MW energy which is sent out by the sensor itself. Passive MW sensors are typically designed to sense the earth-atmosphere in two regions of the spectrum. "Imagers" are designed to operate at frequencies which "see through the atmosphere" to the surface of the earth; "sounders" are designed to operate at frequencies which see the energy emitted from various vertical levels in the atmosphere, and do not see the surface. Figure 3 shows the absorption spectrum in the microwave region. The SSM/I is an imager, and hence, this paper will focus on the imaging capabilities of passive MW sensors.

In approximate form, the satellite measurement, or brightness temperature, TB, at a particular frequency, ν, and polarization[2], p, consists of three terms:

$$TB_{\nu,p} = \underset{\textit{term A}}{T_u} + \underset{\textit{term B}}{\tau_\nu \left[\varepsilon_{\nu,p} T_s\right]} + \underset{\textit{term C}}{\left(1 - \varepsilon_{\nu,p}\right) T_d} \quad (1)$$

where T_u is the upwelling atmospheric emission, τ is the atmospheric transmittance (which is the fraction of energy which emerges at the top of the atmosphere from the surface), T_s is the surface temperature, $\varepsilon_{\nu,p}$ is the emis-

[2] Microwave energy can be described as a two-dimensional wave of energy propagating through space, and commonly consists of a vertical (V) and horizontal (H) component orthogonal to the direction of movement.

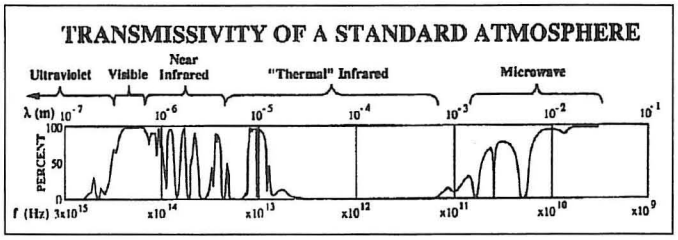

Fig. 2. Electromagnetic Spectrum (from Janssen 1993).

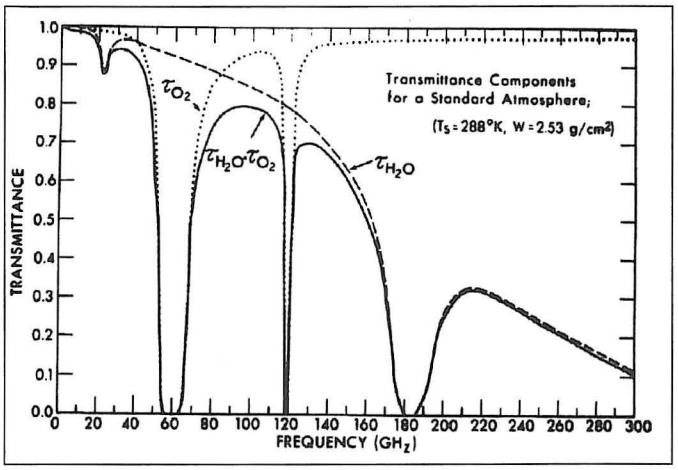

Fig. 3. Microwave transmittance spectrum in a tropical atmosphere (from Janssen 1993).

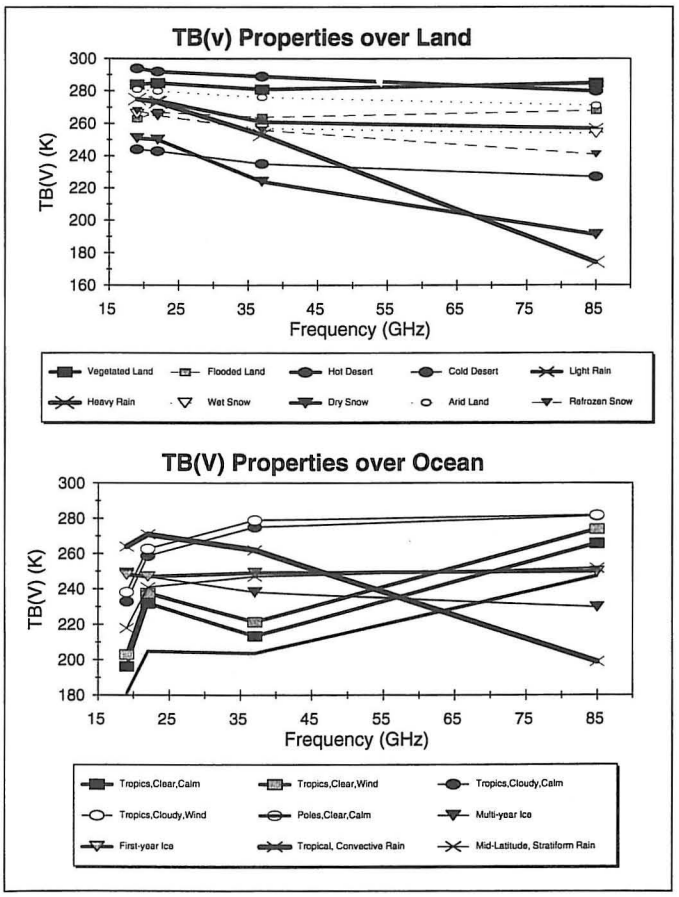

Fig. 4. Emissivity characteristics of various surface types over land (top) and ocean (bottom) represented as 'typical' brightness temperatures as a function of frequency.

sivity (explained below), and T_d is the downwelling atmospheric emission. "Term A" is controlled by the conditions of the atmosphere, which would include the water vapor content, the ice and liquid water content of clouds, etc. At frequencies less than 200 GHz, the effect of cirrus clouds is negligible. "Term B" is controlled by the surface characteristics, which are a function of the observation frequency and polarization. Unlike the IR, where clouds and surfaces are "black bodies" (e.g., they absorb and emit the same amount of energy), surfaces at MW wavelengths generally are "gray bodies" and are not perfect emitters. This property is termed "emissivity", and is one of the major contributors to the TB measured by the satellite. The emissivity properties of various surface types is shown in Fig. 4, which shows the net effect of emissivity on TB through primarily "term B," particularly over land. Finally, "Term C" is the amount of energy, emitted by the atmosphere, that is reflected by the surface, and emitted back through the atmosphere. By assuming that $T_u = T_d = T_s (1 - \tau_\nu)$, equation (1) transforms to:

$$TB_{\nu,p} = T_s (1 - \tau_\nu) + \tau_\nu [\mathcal{E}_{\nu,p} T_s + (1 - \mathcal{E}_{\nu,p}) T_s (1 - \tau_\nu)] \quad (2)$$

As shown in Fig. 4, the large difference in TB between land and ocean is due to a large difference in $\mathcal{E}$. Hence, over ocean, where $\mathcal{E}$ is low, the contribution of the atmosphere is greater relative to the surface contribution. Conversely over land, where $\mathcal{E}$ is much higher, the atmospheric contribution, although similar in magnitude to that over ocean, has less relative weight to TB when compared to the much larger surface contribution. This property controls which parameters can be retrieved over land and ocean.

To further illustrate this concept, assume that the same "atmosphere" exists over a land and water surface, which has a surface temperature of 300 K. Also assume that the $\mathcal{E}$ of land is 0.9 and that of water is 0.5, and the transmittance is 0.9. The resulting TB measured by the satellite, broken into the three terms shown in equation (1) and calculated via (2) would be:

Land: TB = 30 + 243 + 2.7 = 275.7 K
Ocean: TB = 30 + 135 + 13.5 = 178.5 K

As can be seen, the TB over land is much higher, and the relative contribution of the atmospheric signal is approximately 12% over land, and about 25% over ocean.

It should be noted that the radiative transfer is a bit more complicated than this, especially when clouds and rain are present in the atmosphere, and the surface is covered by snow and ice. In these conditions, "scattering" occurs, which essentially reduces the transmittance. For those who would like to pursue the explicit details of microwave radiative transfer, Liou (1980) offers a detailed formulation of these concepts. For those who are interested in the application of these concepts to actual satellite measurements, see Janssen (1993).

b. Example SSM/I measurements

To further illustrate many of the concepts discussed in the previous section, images of SSM/I measurements

taken at 19 GHz and 85 GHz, vertical polarization, are shown in Figs. 5 and 6 (see page 18). These figures show an entire day of measurements taken from the ascending orbits, which is approximately 1800 LST for the F-13 satellite. The most striking feature is the large TB contrast between land and ocean, particularly at 19 GHz. This is due to the lower ε of water compared to land. The effect is not as dramatic at 85 GHz since the ε difference between land and water is not as large at this frequency. Over the oceans, various cloud band features associated with frontal systems are apparent, as well as changes in TB due to the presence of sea ice. Over land, very cold regions are evident on the 85 GHz image. These are associated with the scattering properties of convective rainfall and snowcover, which cause a marked decrease in the TB.

3. Applications and Operational Use

The operational SSM/I retrieval algorithms are designed to utilize the MW window channels and properties to retrieve a host of products, which are described in Table 2. In order to meet operational requirements (i.e., processing multiple satellites, 14 orbits/day/satellite, optimal processing time, etc.), the current operational algorithms run at the US Navy's Fleet Numerical Meteorology and Oceanography Center (FNMOC) are statistical, or empirical, in nature. This means that the channels used in the retrievals come from theoretical considerations, but they are tuned with ground data rather than model derived coefficients.

Table 2. SSM/I Environmental Data Records (EDR), produced operationally at FNMOC.

EDR Product name	Range/units
Cloud Liquid Water	0 - 1 kg/m2
Rain Rate	0 - 35 mm/hr
Wind Speed	3 - 25 m/sec
Soil Moisture	0 - 60 %
Ice Concentration	0 - 100 %
Ice Age	First/Multiyear
Ice Edge	Ice/No Ice
Total Precipitable Water	0 - 80 kg/m2
Snow Water Equivalent	0 - 50 cm
Surface Type	~ 20 Types
Surface Temperature	180 - 340 K

a. Total precipitable water

The integrated water vapor, also known as total precipitable water (TPW), can be retrieved by utilizing measurements near the center of a weak water vapor absorption line at 22 GHz (Fig. 3). By combining these measurements with channels at other frequencies, the effects due to clouds, rain, and surface wind are minimized. Retrievals over land are not possible at this frequency due to the high and variable emissivity over land surfaces. Since most of the moisture is in the lower atmosphere, below 700 mb, these retrievals are strongly coupled with sea-surface temperature, especially over the tropical oceans (Stephens 1990). The TPW is one of the most accurate parameters retrieved by passive microwave sensors, with errors of approximately 10% when compared with radiosonde measurements (Alishouse et al. 1990). The current operational SSM/I algorithm is a modified version of the Alishouse et al. (1990) algorithm (with a cubic correction to account for biases at low and high TPW values) and uses a combination of the TB's at 19V, 22V and 37V, including a quadratic term at 22V.

The TPW product is used to complement conventional meteorological and subjective/human interactive NESDIS techniques for the analysis and forecast of precipitation (Scofield 1993). This product has been useful for precisely locating concentrations of moist low level air, one of the most important ingredients necessary for generating and sustaining heavy precipitation (Kusselson 1993). The concentrations of high precipitable water values is better known as the TPW plume. Many times, especially in the cool seasons, the TPW plume originates in the subtropical/tropical regions of the Atlantic and Pacific oceans. The surges of moisture associated with the TPW plume can be seen at least 1-2 days in advance of the actual precipitation event and are a well-defined satellite signature of heavy precipitation potential. In addition, several years of research by the NOAA/NESDIS/Satellite Analysis Branch (SAB) have shown a strong correlation between the 1-2 km height winds parallel the TPW plume and increased precipitation efficiency of the plume. Other necessary ingredients for maximizing precipitation efficiency and leading to heavy precipitation at a particular location are the analysis of middle level troughs and jet streams from the GOES IR 6.7 micron water vapor channel. In this way, the SSM/I TPW product compliments the various GOES channels and makes for a more accurate satellite analysis of the location and potential for heavy precipitation. Since 1992, the NESDIS/SAB has operationally incorporated the SSM/I TPW composite product into their overall satellite analysis and forecasts for the joint NCEP/NESDIS National Precipitation Prediction Unit (NPPU). The analyses and short term forecasts are provided through briefings to the NCEP Hydrometeorological Prediction Center (HPC) and heavy precipitation messages (AFOS header NFDSPENES) to River Forecast Centers and Weather Forecast Offices of the National Weather Service. Through these briefings and messages, the SSM/I TPW product is being used at the national and local levels as value added products to identify heavy precipitation potential up to 48 hours in advance.

Illustrated in Fig. 7 is an example of the SSM/I TPW composite product of F-13 and F-14 ascending orbits for a 18-hour period ending on 1200 UTC 11 December 1997. Well defined frontal features can be seen across the Atlantic and Pacific Oceans. The most striking feature is the concentration of high TPW (e.g., TPW plume) streaming from the tropical Pacific (east of Hawaii) northward to British Columbia. The advection of this moisture and the degree to which it connects to the tropical moisture and

mid-latitude upper level destabilizing features ultimately determines how intense the rainfall will be over land.

b. Rain rate

Rainfall affects earth emitted MW radiation in two ways: absorption by rain drops, and scattering by ice particles. Because of the low $\mathcal{E}$ of the ocean surface, the absorption/emission signature caused by rain drops (i.e., increase in TB) is easily detected, while this feature is virtually impossible to detect over the "warmer" land surface. Low frequency measurements are best suited for the emission technique. The scattering property is most prevalent at high frequencies and is caused by particles that are comparable in size to the wavelength of energy being measured. At 85 GHz, this translates to a particle size of about 4 mm or greater. In the rain layer, there is a mixture of snow, ice and rain particles (sometimes called graupel) and this is the main cause of the scattering. This affect is detected by a decrease in TB in the active raining regions. Scattering is detectable over both land and ocean.

The operational SSM/I rainfall algorithm utilizes a "scattering index" (Grody 1991) over land and ocean, which is simply the difference between the estimated 85 GHz measurement in the absence of scattering and the actual TB_{85V}. Care must be taken to account for other scattering signatures which can resemble rain (see Fig. 4). In particular, cases of melting snow, that are typical after a full day of melting in the 1800 and 2200 LST SSM/I overpasses, can cause false rain signatures. In addition to the scattering signatures, an emission component of rain is used over the ocean using the liquid water path (LWP) algorithm of Weng and Grody (1994). Rain rates are determined using relationships developed with co-incident radar data (Ferraro and Marks 1995). As determined from their study, the minimum detectable rain rate over land is about 0.5 mm h^{-1} while over ocean it is approximately 0.2 mm h^{-1}. A complete description of the algorithm is given in Ferraro (1997).

The rain rate product is used by NESDIS/SAB to locate areas of rain/no-rain and light/moderate/heavy rain rates. It is particularly useful over the data sparse ocean areas. One way the SSM/I rain rate product complements other satellite data is when it is overlaid on the same time GOES imagery. In this way, the SAB analyst can identify which parts of the IR/visible cloud band are producing rain and the heaviest rain rates. This provides valuable information to:

1) confirm the onset of steady precipitation,
2) forecast the duration of steady precipitation, and
3) locate the highest precipitation rates and potential for significant precipitation amounts.

In addition, for the past few years NESDIS/SAB has used the SSM/I rain rates to produce an experimental rainfall potential for tropical storms. This rainfall estimate uses the objective SSM/I rain rates through the storm to produce a rain width area (km) and an average rain rate (mm h^{-1}). Incorporating the tropical storm's speed (km h^{-1}) into the calculations results in the rainfall potential. Rainfall potentials for tropical storms expected to make landfall within 24 hours have been provided to the NCEP Hurricane Prediction Center (HPC) and Tropical Prediction Center (TPC) as guidance in their precipitation forecasts. The experimental rainfall potential product has recently been expanded to include tropical storms in the eastern hemisphere and the faster moving winter storms that affect the United States.

Figure 8 shows the composited SSM/I derived rain rate fields for the same time period as that shown in Fig. 7. Rainfall associated with mid-latitude frontal systems are evident over the Pacific and Atlantic oceans. Convective rain clusters over the tropical Pacific ocean show some of the heaviest rain rates (in excess of 20 mm h^{-1}). Melting snow in the Great Plains is misclassified as falling rain and is a subject of continued fine-tuning of the SSM/I algorithms at the NESDIS/ORA.

c. Ocean surface wind speed

Clear, calm ocean surfaces have very low $\mathcal{E}$ values. Winds act on the ocean surface and generate both foam and millimeter sized capillary waves, both of which act to "roughen" the ocean surface at MW wavelengths and hence, increase the $\mathcal{E}$. It is possible to detect these changes under rain free conditions. On the SSM/I, the 37 GHz channels appear to be best suited to detect these changes, although other channels are used to minimize the effects of cloud cover and water vapor. The current operational SSM/I algorithm is a modified version of the Goodberlet et al. (1989) algorithm (with an adjustment for high values of TPW) and uses the 19V, 22V, 37V and 37H channels. Accuracies vary with the amount of atmospheric contamination, but are on the order of 2-5 m s^{-1}. Passive microwave sensors cannot retrieve wind direction. Scatterometers, like the one on the European Remote Sensing Satellite (ERS-2), can retrieve wind vectors.

The NCEP/Marine Prediction Center (MPC) is responsible for issuing wind warnings over the North Atlantic from 32 to 65 degrees north, west of 35 degrees west, and over the Pacific east of 160 degrees east from the Bering Strait to 30 degrees north. MPC high seas wind warnings are in bulletin format and MPC graphical analysis/forecasts are distributed directly to vessels at sea via US Coast Guard marine radiofacsimile broadcasts. The SSM/I wind speed (and precipitation) data gives the MPC forecaster a more complete picture of both wind field distribution and frontal structure of mid-latitude cyclones. The SSM/I information is more detailed than that provided by conventional synoptic observations and satellite imagery. The use of SSM/I data has led MPC forecasters to embrace recent theories concerning cyclone frontal structures and wind field distributions. SSM/I wind fields have helped forecasters make educated adjustments to numerical wind and ocean wave forecast fields.

NESDIS/SAB utilizes the SSM/I wind speed product to provide information in the relatively data sparse ocean areas. It is used to supplement GOES satellite low level wind vectors for diagnosing moisture inflow for the generation and maintenance of precipitation. The product is also used by the SAB Tropical Team to complement their geostationary satellite analysis of tropical disturbances.

Shown in Fig. 9 is an example of the SSM/I wind speed

product for the same time period as the previous two figures. The changes in wind speed associated with various high and low pressure systems are clearly evident.

d. Snow and sea-ice cover

Snow cover and sea-ice were first derived from passive microwave measurements in the early 1970's (e.g., Kunzi et al. 1976; Zwally and Gloersen 1977). Snow cover has a scattering signature similar to that of falling rain. The two can generally be separated by using a simple threshold at a low frequency channel like 22 GHz (Grody 1991). Snow cover retrieval algorithms have been improved utilizing the 85 GHz measurements from the SSM/I to detect shallow snow cover and screen the measurements for false signatures (i.e., rainfall, frozen ground, and cold deserts). The current operational SSM/I snow detection algorithm was developed by Grody and Basist (1996), and utilizes the scattering at both 37 and 85 GHz to detect snow on the ground. The screening techniques use a wide variety of channel combinations.

Sea-ice causes an increase in emissivity over that of open water, and forms the basis for the retrieval algorithm. Sea-ice concentration is retrieved using a combination of measurements at 19 and 37 GHz and at both polarizations. The current operational algorithm is described in Hollinger (1991).

The SSM/I snow cover and sea-ice concentration products are used operationally by NESDIS/SAB to supplement satellite VIS and IR imagery. The SAB utilizes all of the satellite data in their production of a daily Northern Hemisphere snow/ice map. The SSM/I products are useful in cases where recent snow fall is masked by cloud cover and over high latitude areas in the winter season when there is no sunlight to utilize VIS imagery.

e. An example of multisensor use

This section illustrates a "typical" example of how GOES and SSM/I data products are used to assess the precipitation potential of a system affecting the west coast of the United States. Shown in Fig. 10 is the GOES imagery for Channels 1, 3, and 5 (i.e., 0.65 micron visible, 6.7 micron water vapor, and 12 micron IR, respectively) for 1700 UTC 8 February 1998. At that time, several low pressure systems were affecting the west coast of the

ZCZC NFDSPENES ALL DDHHMM;390,1220 340,1190 340,1210 390,1240;
TTAA00 KNFD DDHHMM

SATELLITE PRECIPITATION ESTIMATES...DATE/TIME 2/8/98 1930Z
THE SATELLITE ANALYSIS BRANCH/NESDIS—NPPU— TEL.301-763-8678
VALUES ARE MAX OR SGFNT EST. NO OROGRAPHIC CORRECTION UNLESS NOTED.
...EST'S FM: /GOES8-CNTRL AND E. U.S. / GOES9 - W. U.S...
REFER TO TPB#375 FOR DETAILS. LATEST DATA USED: GOES-9 1900Z SJK
SSM/I 1710Z
LOCATION... CNTRL CA/S CA...SEE GRAPHIC FOR AMTS....
.
REMARKS FOR CA...LATER SSMI PASS AT 1710Z WIDTH OF RAIN BAND AVGING ABOUT 1 DEG AND CNTRD FROM 32N/127W TO 35N/124W TO 37N/124W... CURLING NWWD TO 38N/125W. GENERAL RAIN RATES CONTINUE BELOW 0.1"/HR ...HOWEVER THERE WERE SOME ISOLATED POCKETS OF NR 0.15"/HR AT 33.5N/125W (HEADING FOR SOUTHERN CA) AND 36N/124W AND 38N/125W HEADING FOR CENTRAL AND N CA...THESE RATES ARE ABOUT THE SAME AS 14Z SSMI PASS AND MUCH WEAKER/LOWER THAN YDYS STORM. NOT TOO MENTION ALSO THAT 700MB TRANSPORT WINDS ONLY BLOWING A SHT DISTANCE PARALLEL TO THE BEST MOISTURE WITH FRONT...SO EVEN MORE REASON TO EXPECT QUICKER AND MUCH LESS PRECIP BOTH NORTHERN TO CENTRAL CA NXT SEVERAL HRS AND SOUTHERN CA LATER TODAY AND EVE...IN-HOUSE RAINFALL POTENTIAL USING SSMI RAIN RATES GIVING UP TO 0.5" PER 6HRS OF NON OROGRAPHIC PRECIP. LATEST GOES VIS SHOWING GOOD BURST IN S SAN MATEO COUNTY INTO N SANTA CRUZ AND WILL BE AFFECTING SANTA CLARA NXT HR OR SO...THIS GOOD BURST COULD GIVE UP TO 0.5"/HR AS IT MOVES BY...ADDTIONAL BURSTS JUST OFFSHORE KMRY AND KSFO COULD GIVE LOCALLY HVY BUT RELATIVELY BRIEF HVY RAIN BY 22-23Z. LEADING EDGE OF LT TO MODERATE RAIN HEADING INTO SANTA BARBARA BY 22Z AND CONTINUING THRU AT LEAST 00Z THERE. WILL CONTINUE TO MONITOR....
.
G9 MOTOR WINDING OPERATIONS HAVE STARTED FM NOW TIL MARCH 1. MOST OF DATA FM 0430 TO 1200Z WILL BE MISSING. G8 DATA IS STILL AVLBL DURING THAT PERIOD....ALONG WITH THE EVENING PASSES OF SSMI MICROWAVE DATA.
.
SATELLITE ESTIMATE GRAPHIC FOR THE PERIOD 16-19Z ON INTERNET AT THE ADDRESS BELOW...OROGRAPHICS INCLUDED
.
PLEASE SEE HPC QPF DISCUSSIONS AND GRAPHICS FOR DETAILS OF FORECAST PRECIP AMOUNTS.
.
http://www.ssd.noaa.gov/SSD/ML/pcpn-ndx.html
[ONLINE SSD PRECIPITATION PRODUCT INDEX]

United States, as depicted by the GOES imagery and surface weather charts (not shown). One system was centered across the intermountain region of Utah and Arizona, with a trailing frontal system extending southwestward into Baja California and into the Pacific ocean. Another system was centered just off the northern California coast (1010 mb low) and extending southward along almost the entire California coast. Note the strong mid-level drying behind this system as depicted in the GOES water vapor imagery. A final, very deep system (995 mb), was centered just off the Washington coast.

In order to estimate the intensity and duration of the precipitation, information on the rain rates and moisture inflow are needed. Since a portion of the active rain system is still offshore of the California coast (and out of radar range), the SSM/I rain rate product is useful (Fig. 11). Here, rain rates on the order of 5 mm h^{-1} or less are seen for all three systems. It should be noted that the GOES imagery was selected to closely correspond to the overpass time of the SSM/I observations along the California coast. As was previously described, the TPW helps determine the potential for prolonged and heavy rainfall episodes. If a forecaster were to rely solely on the GOES derived TPW (Fig. 12), estimates are restricted to cloud-free areas and hence, are limited in use. (However, these estimates are available over land, which are not available from the SSM/I). Using the SSM/I derived TPW (Fig. 13), the advection of moisture plumes are apparent, and are more prevalent with the southern most system. In fact, devastating flooding occurred in northern Mexico as a result of this rain band.

As previously described, NESDIS/SAB provides heavy precipitation messages through a variety of mechanisms. Shown on page 16 is one example of these messages which corresponds to the case study described in Figs. 10-13.

4. Discussion

The era of passive microwave remote sensing has allowed for the development and application of retrieval algorithms for assessing rainfall potential, improving marine warnings, and probing through clouds to map snow and ice cover. These products offer excellent complements to "conventional" satellite imagery and ground measurements, and provide "value added" information to the weather forecaster. It is anticipated that the uses of these derived products will greatly increase over the next several years, as NWS field offices have only recently begun to recognize its potential through the access of the products (through RAMSDIS and the World Wide Web). In addition, researchers at the NESDIS/ORA are beginning to develop multisensor products of TPW and rainfall (derived from GOES and SSM/I measurements) which will offer the user community products which blend the "best" attributes of the various individual components. At present, the operational SSM/I products (e.g., Environmental Data Records) are only available through NOAA/NESDIS, FNMOC, and

Table 3. Internet World Wide Web sites containing MW data in quasi-operational mode (as well as other interesting satellite information).

Web Site	Address	What's There
NOAA/NESDIS/ORA	http://orbit35i.nesdis.noaa.gov/arad/ht	Description of ORA activities, with links to SSM/I images, etc.
NOAA/NESDIS/ORA Hydrology Team, Microwave Sensing Group	http://orbit35i.nesdis.noaa.gov/arad2	Access to imagery of daily SSM/I and AMSU channel measurements, monthly climate products, and case studies
NOAA/NESDIS/ORA Ocean Physical Processes Team	http://manati.wwb.noaa.gov/ssmiwind.html	Ocean wind speeds, TPW, and rain rates, updated every 6 hours. Loops of daily mean SSM/I products.
NOAA/NESDIS/ORA Hydrology Team	http://orbit35i.nesdis.noaa.gov/arad/ht/ff/swi.html	Soil wetness and anomalies
NOAA/NESDIS/OSDPD Shared Processing	http://psbsgi1.nesdis.noaa.gov:8080/PSB/SHARED-PROCESSING	Access to SSM/I products received from FNMOC
NCDC	http://www.ncdc.noaa.gov/ol/satellite/ssmi/ssmiproducts.html	Access to archived global monthly products
NGDC	http://www.ngdc.noaa.gov/dmsp/dmsp.html	Access to archived DMSP data, case studies, and good background information
CIRA	http://amsu.cira.colostate.edu/	Access to AMSU products
NOAA/NESDIS/ORA/ RAMM Team	http://www.cira.colostate.edu/ramm/rmsdsol/main.html	Online access to the RAMSDIS system
NOHRSC	http://www.nohrsc.nws.gov	Access to SSM/I snow cover products

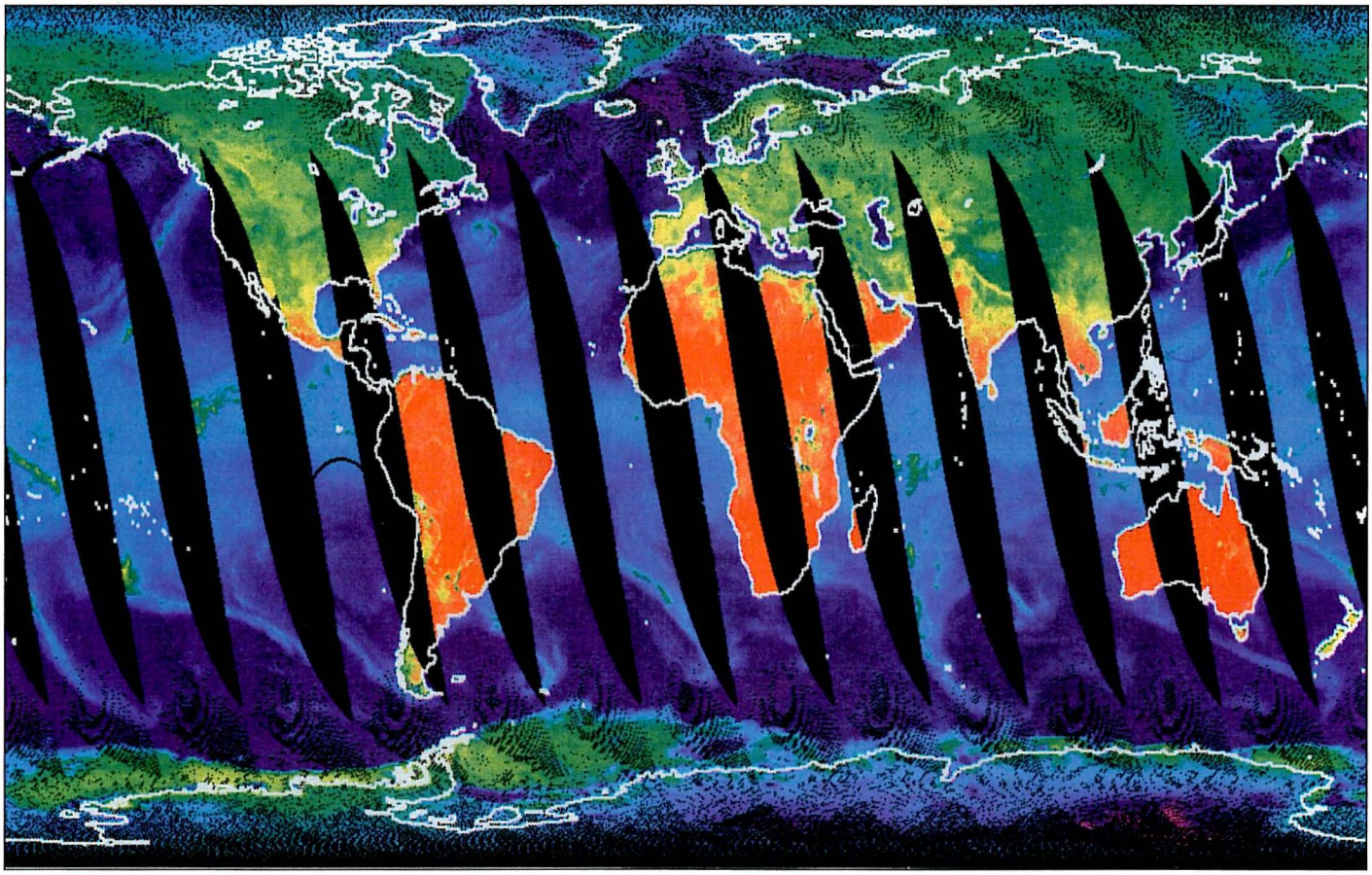

Fig. 5. SSM/I F-13 ascending orbits for 11 December 1997, for measurements taken at 19 GHz (vertical polarization). TB's range from 160 K (purple) to 290 K (red).

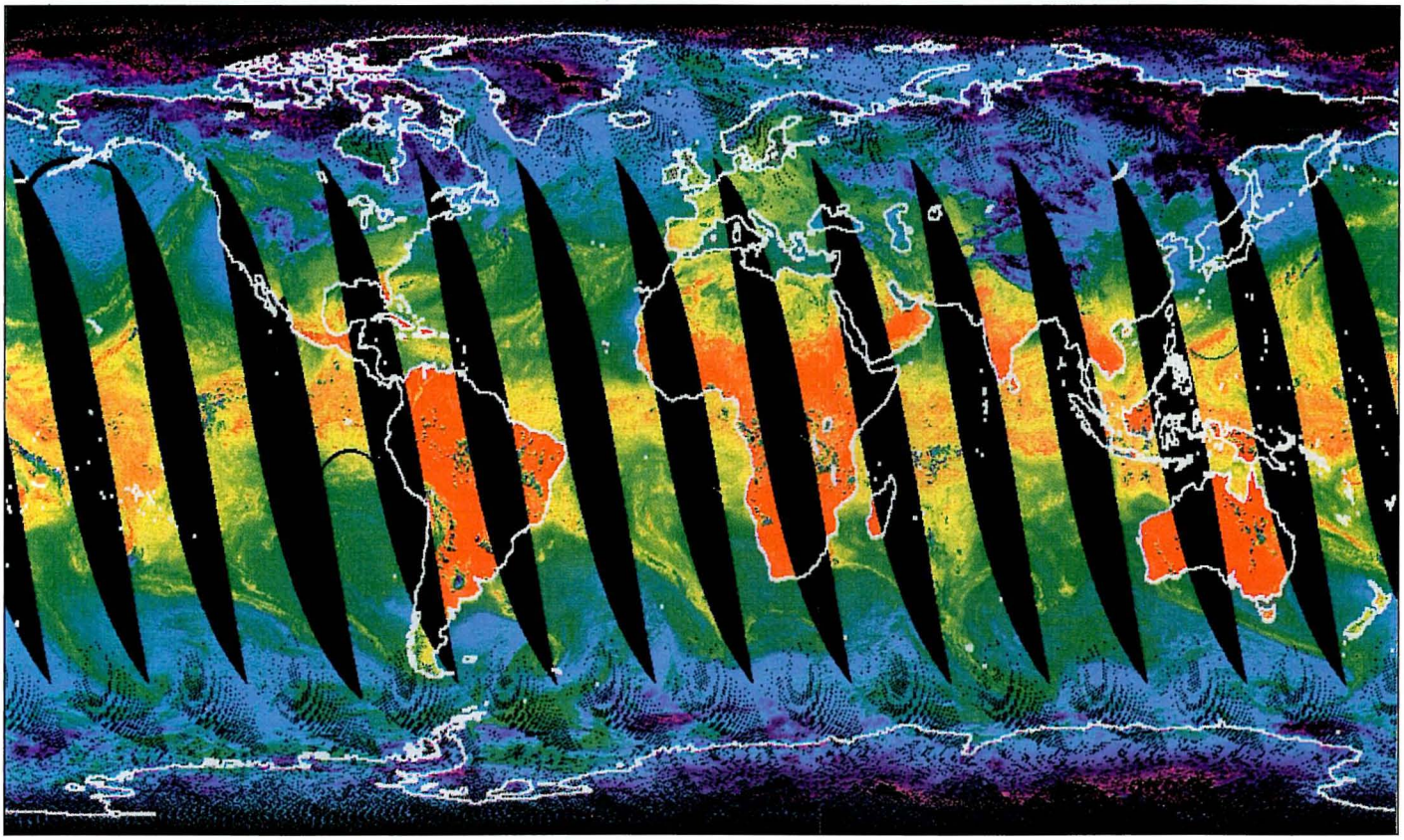

Fig. 6. As in Fig. 5, but for the 85 GHz (vertical polarization) channel.

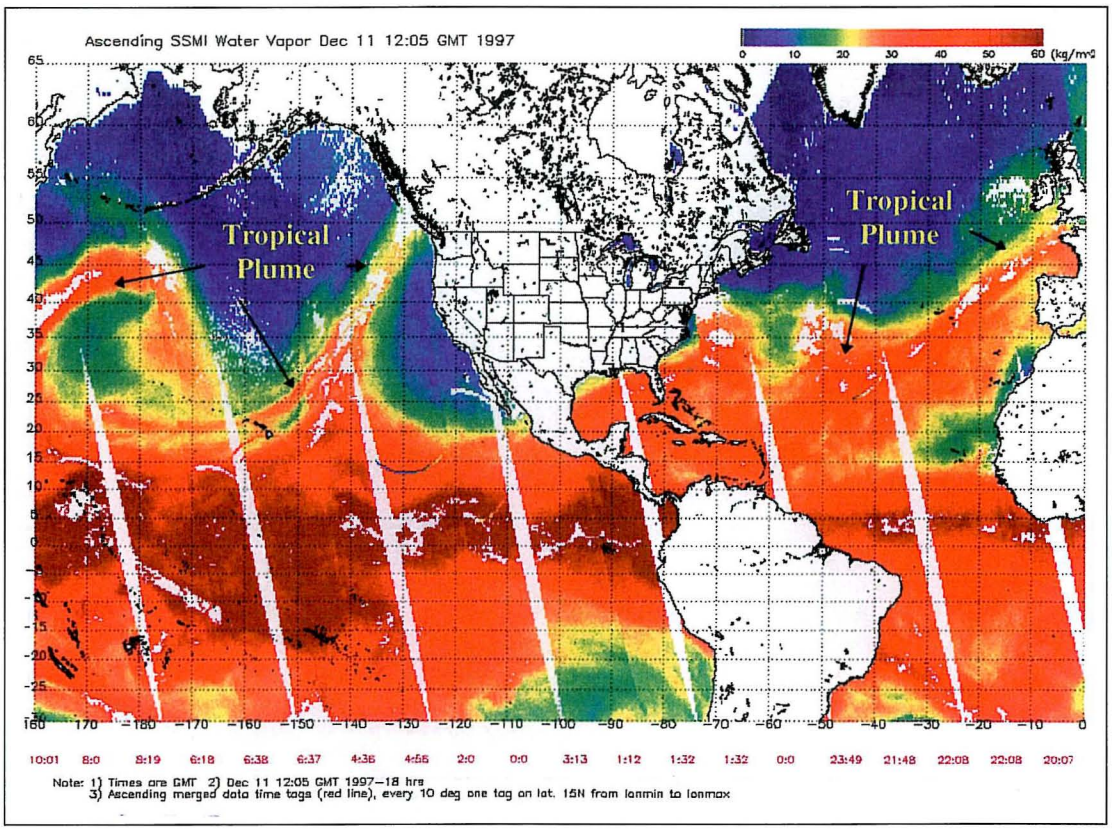

Fig. 7. A composite of SSM/I F-13 and F-14 ascending orbits, showing TPW retrievals for all available orbits for an 18-h period ending 1200 UTC 11 December 1997. Units and colors are denoted in the color bar, and the approximate times of the overpasses are shown below the image. Areas of active rain over the ocean are depicted as white and no TPW retrievals are made when rain is present.

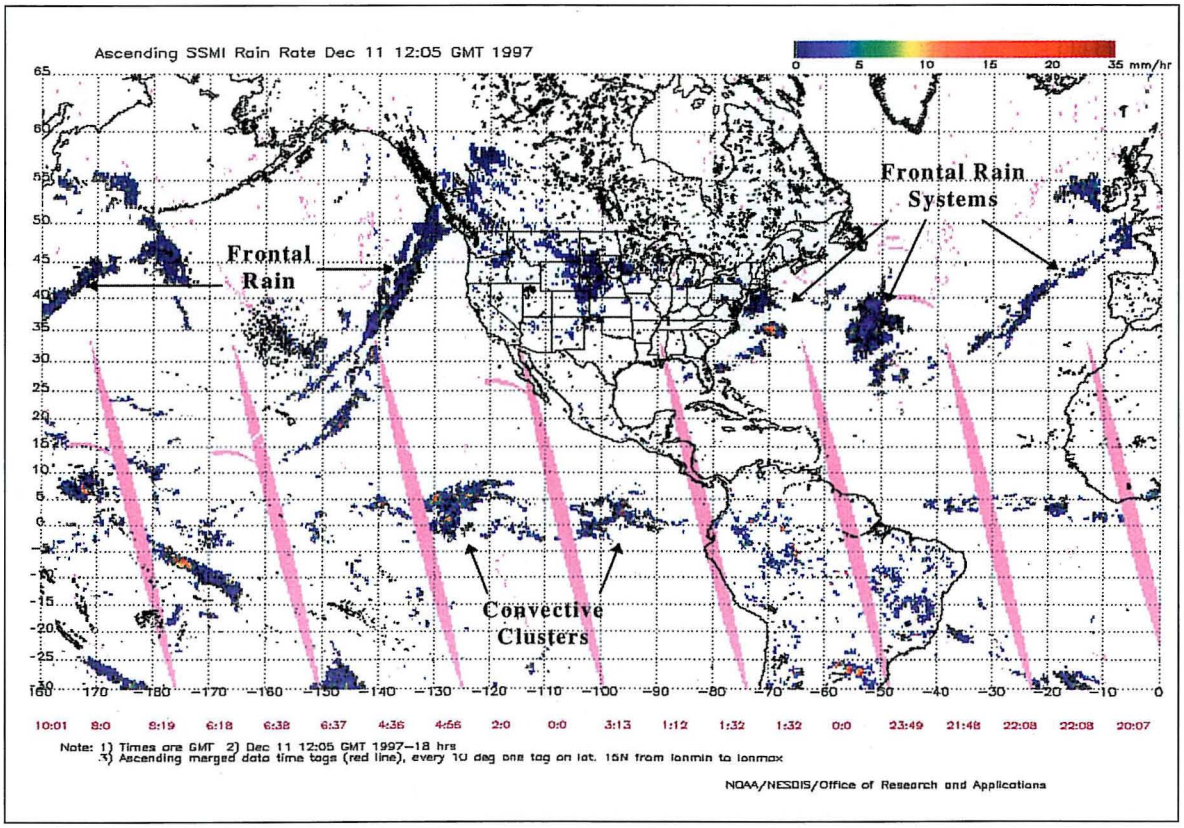

Fig. 8. A composite of SSM/I F-13 and F-14 ascending orbits, showing rain rate retrievals for an 18-h period ending 1200 UTC 11 December 1997. Units and colors are denoted in the color bar, and the approximate times of the overpasses are shown below the image.

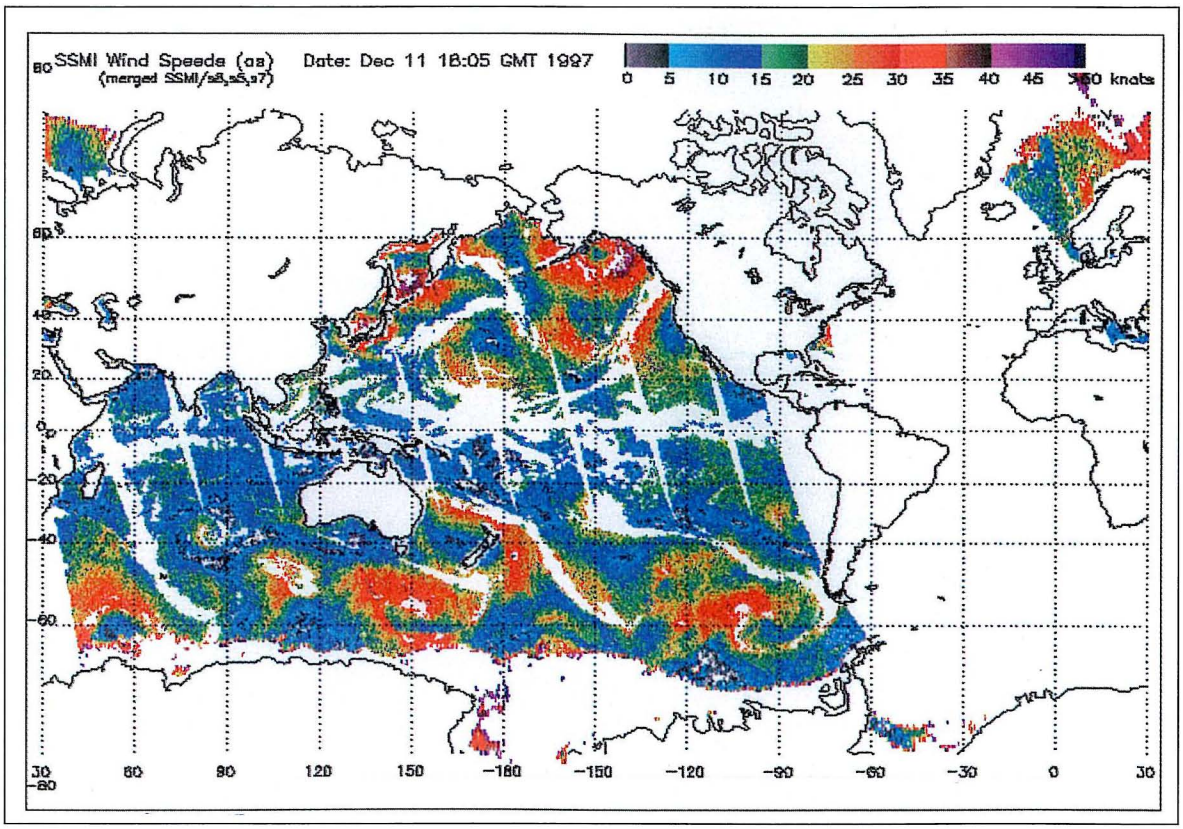

Fig. 9. A composite of SSM/I F-13 and F-14 ascending orbits, showing wind speed retrievals for all available orbits for an 18-h period ending 1800 UTC 11 December 1997. Units and colors are denoted in the color bar. White regions within the orbital swaths are regions where wind speed was not retrieved due to the presence of high atmospheric contamination due to dense clouds and precipitation.

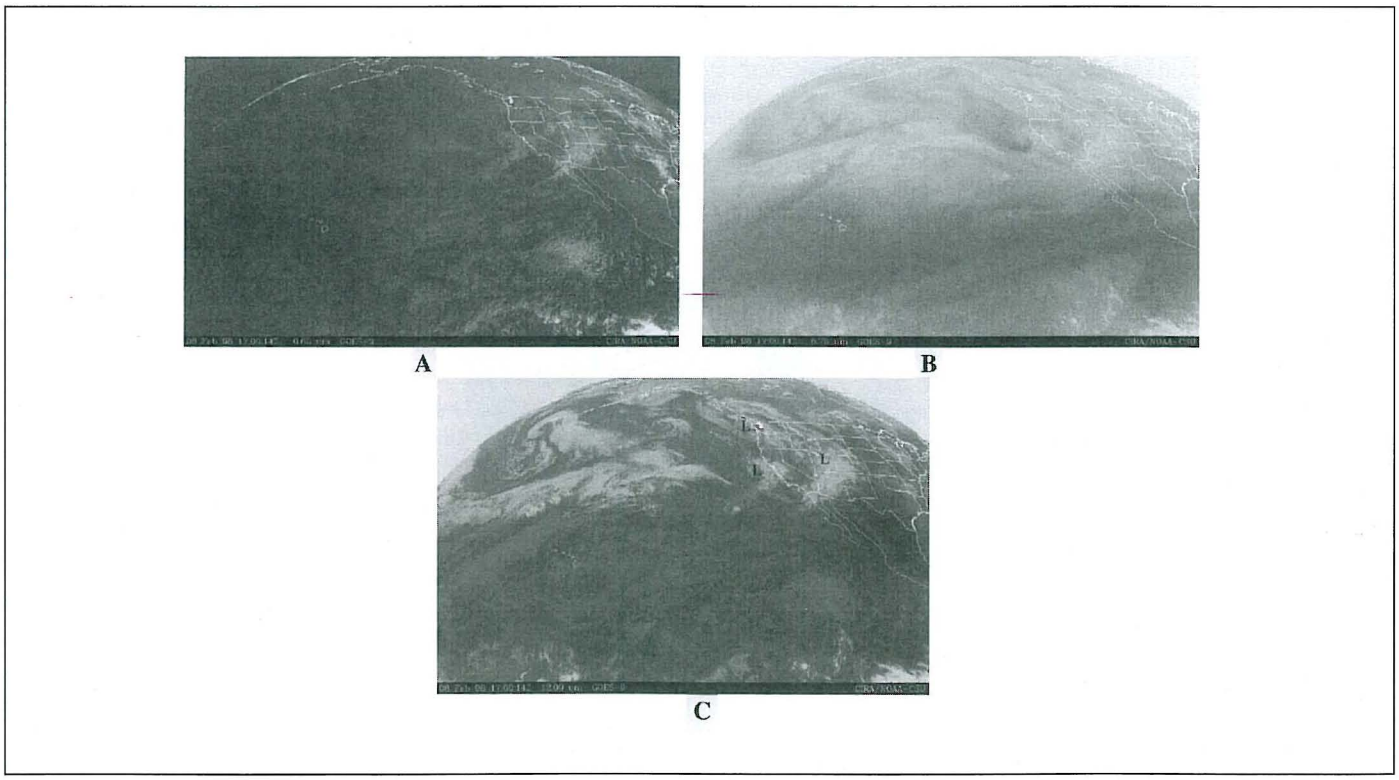

Fig. 10. GOES imagery 1700 UTC 8 February 1998: (A) Channel 1 visible, (B) Channel 3 water vapor, and (C) Channel 5 IR.

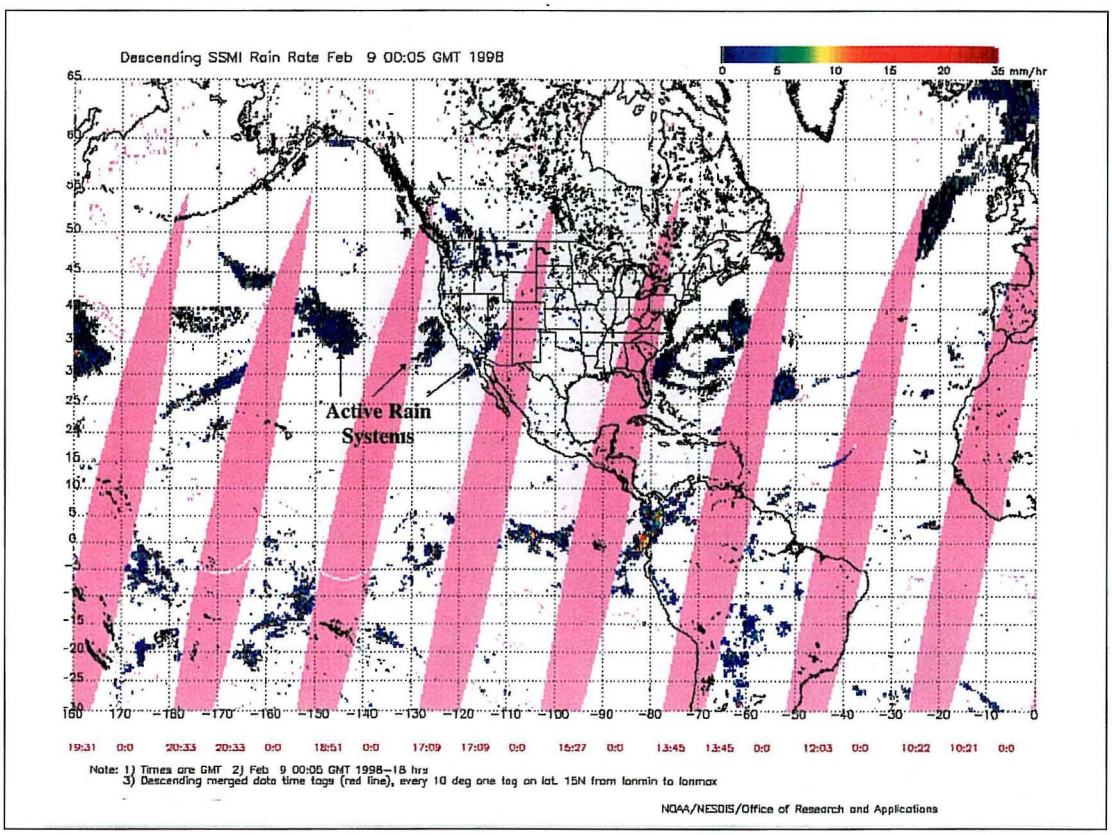

Fig. 11. As in Fig. 8, but for descending orbits for an 18-h period ending 0000 UTC 9 February 1998.

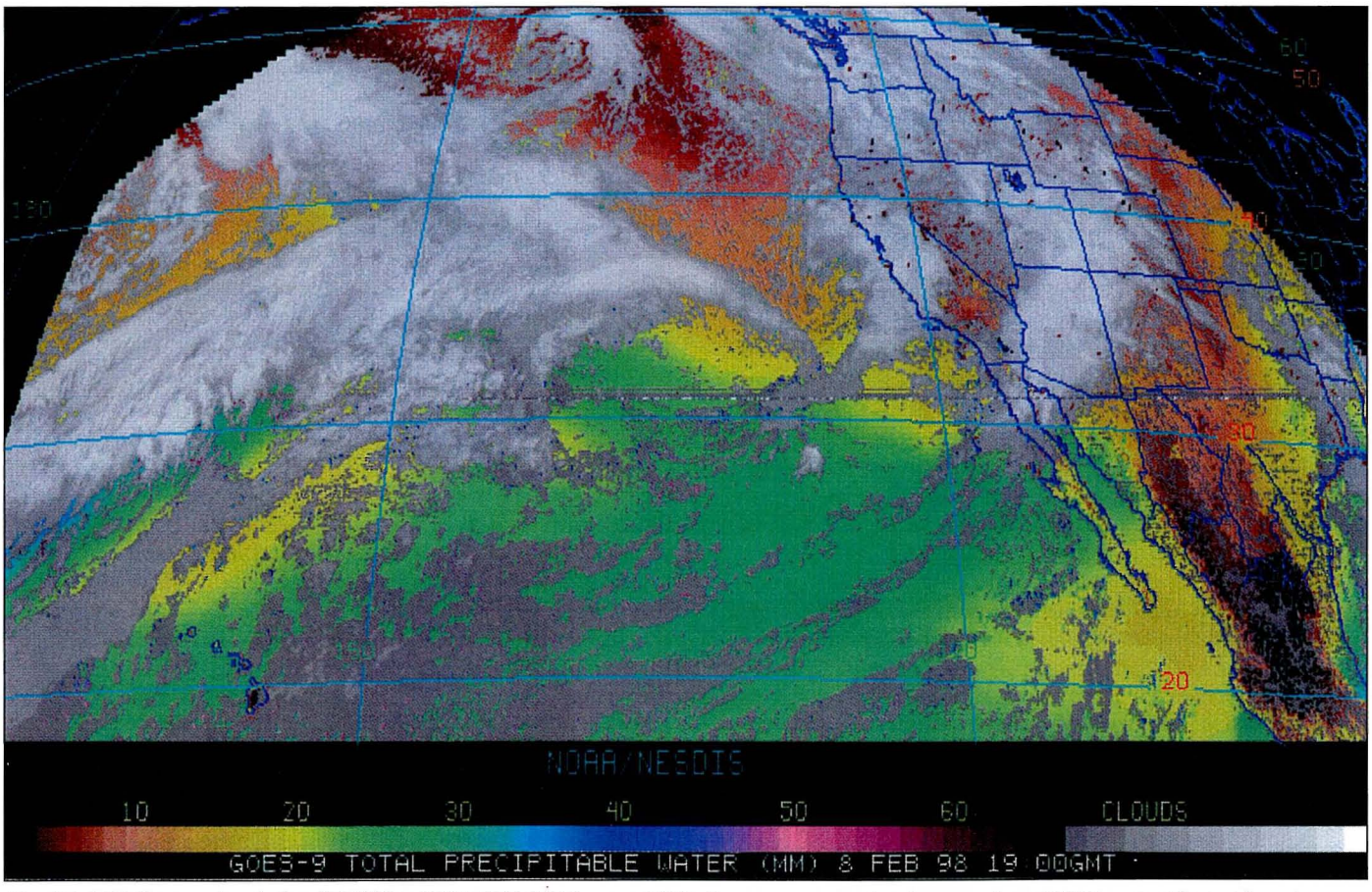

Fig. 12. GOES sounder derived TPW for 1900 UTC 8 February 1998. Gray areas are cloud covered and TPW cannot be retrieved.

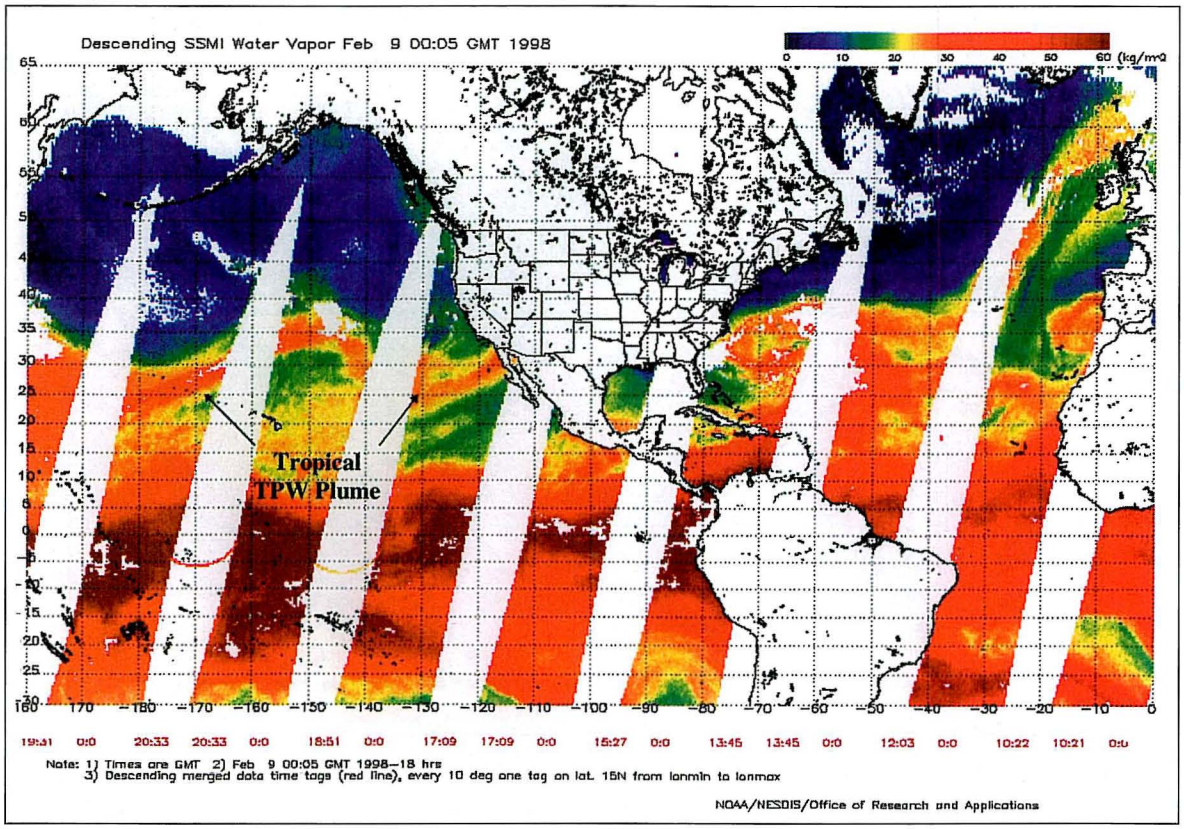

Fig. 13. As if Fig. 7, but for descending orbits for an 18-h period ending 0000 UTC 9 February 1998.

through the RAMSDIS system. Table 3 details some World Wide Web sites which will allow for the accessing and/or viewing of SSM/I data, although in a less timely fashion.

The future of passive microwave remote sensing will include several operational and research sensors. These sensors will lead to improvements over the current operational algorithms. The recently launched NOAA-15 satellite (May 1998) contains a new sensor called the Advanced Microwave Sounding Unit (AMSU). At the time of this writing, the sensor is undergoing final evaluation. Although the AMSU is a "sounder", it contains several window channels between 23 and 150 GHz that will allow NESDIS to generate a product suite similar to that of the SSM/I. There are some significant differences in the sensor designs of the SSM/I and AMSU which are beyond the scope of this paper. Nonetheless, it is anticipated that a product suite of comparable quality to those generated by the SSM/I will be available to the scientific community by the end of 1998.

There are also a series of sensors that are not "operational", but will be available for research and development activities. These sensors may provide the best quality measurements ever taken in the passive MW spectrum. These include measurements from Tropical Rainfall Measuring Mission (TRMM) Microwave Imager (TMI) aboard the NASA TRMM satellite, the Advanced Microwave Scanning Radiometer (AMSR) aboard the Japanese ADEOS-II satellite and the NASA EOS-PM 1 satellite. The TRMM was launched in November 1997, while the ADEOS-II and EOS-PM will be launched around 2000 or later. The TMI includes measurements at 10.7 GHz and the AMSR at 6.9 and 10.7 GHz. These lower frequencies will allow for the improved retrieval of several parameters, in particular, ocean surface wind speed and rain rate over ocean.

Acknowledgments

The authors would like to acknowledge the contribution of J. Sienkiewicz, NCEP/Marine Prediction Center, who provided the information on the use of SSM/I winds. We also like to thank the efforts of Paul Chang of NOAA/NESDIS and Steve Olson of Research and Data Systems, Corp., who have worked diligently in getting near real-time SSM/I information out in various forms on the World Wide Web, and whose imagery were used in this paper. Also, we extend thanks to the CIRA/NOAA-CSU and NESDIS/FPDT, whose GOES imagery were used in the figures and to Rod Scofield (NOAA/NESDIS) who offered constructive comments to the original manuscript. In addition, we are grateful to Fran Holt of NOAA/NESDIS who "persuaded" us to write this article, and offered constructive reviews during the preparation of this manuscript. Last but not least, we thank the formal reviews of Andy Jones and Rich Grumm, who provided thoughtful comments which greatly improved the final manuscript.

Authors

Ralph Ferraro is a Physical Scientist with the NOAA/NESDIS/Office of Research and Applications in Camp Springs, MD. He is assigned to the Hydrology

Team of the Atmospheric Research and Applications Division. Mr. Ferraro has been working with passive microwave satellite measurements for nearly 15 years, and has published and presented numerous papers on various aspects of this subject, including algorithm development, and applications to weather forecasting and climate monitoring.

Sheldon Kusselson has been an operational satellite meteorologist for the past 19 years with the NOAA/NESDIS/Satellite Services Division of the Office of Satellite Data Processing and Distribution. He has been a member of the Precipitation Team of the Satellite Analysis Branch since 1983 and the microwave data applications focal point since 1991.

Dr. Marie Colton is a program manager for the US Navy's remote sensing research at the Office of Naval Research in Arlington, VA. While at her previous position at the Naval Research Laboratory (Monterey), Dr. Colton's research addressed environmental effects on radar backscatter. She was responsible for the end-to-end processing of the DMSP Special Sensor Microwave/ Imager data at the Fleet Numerical Meteorology and Oceanography Center, which included chairing a multi-agency algorithm research panel.

References

Alishouse, J.C., S. Snyder, J. Vongsathorn and R.R. Ferraro, 1990: Determination of oceanic total precipitable water from the SSM/I. *IEEE Trans. Geo. Rem. Sens.*, 28, 811-816.

Ferraro, R.R., and G.F. Marks, 1995: The development of SSM/I rain rate retrieval algorithms using ground based radar measurements. *J. Atmos. Oceanic Technol.*, 12, 755-770.

_____, 1997: SSM/I derived global rainfall estimates for climatological applications. *J. Geophys. Res.*, 102, 16,715-16,735.

Goodberlet, M.A., C.T. Swift and J.C. Wilkerson, 1989: Remote Sensing of Ocean Surface Winds with the Special Sensor Microwave Imager. *J. Geophys. Res.*, 94, 14544-14555.

Grody, N.C., 1991: Classification of snow cover and precipitation using the Special Sensor Microwave/Imager (SSM/I). *J. Geophys. Res.*, 96, 7423-7435.

_____, and A. Basist, 1996: Global identification of snow cover using SSM/I measurements. *IEEE Trans. Geo. Rem. Sens.*, 34, 237-249.

Hollinger, J., 1991: *DMSP SSM/I calibration/validation. Final report parts I & II.* Naval Research Laboratory, Washington, DC. 419 pp.

Janssen, M. A., 1993: *Atmospheric remote sensing by microwave radiometry*. John Wiley and Sons, Inc., New York, New York, 572 pp.

Kunzi, K.F., A.D. Fisher, D.H. Staelin, and J.W. Waters, 1976: Snow and ice surfaces measured by the Nimbus 5 microwave spectrometer. *J. Geophys. Res.*, 81, 4965-4980.

Kusselson, S.J., 1993: The operational use of passive microwave data to enhance precipitation forecasts. Preprints: *13th Conference on Weather Analysis and Forecasting*, Vienna, VA, Amer. Meteor. Soc. 434-438.

Liou, K., 1980: *An introduction to atmospheric radiation*. Academic Press, Inc., New York, New York, 392 pp.

Scofield, R.A., 1993: The satellite funnel approach for "0-48 hour" weather prediction. Preprints: *13th Conference on Weather Analysis and Forecasting*, Vienna, VA,, Amer. Meteor. Soc. 48-53.

Stephens, G. L., 1990: On the relationship between water vapor over the oceans and sea surface temperature. *J. Climate*, 3, 634-645.

Weng, F. and N.C. Grody, 1994: Retrieval of cloud liquid water using the special sensor microwave imager (SSM/I). *J. Geophys. Res.*, 99, 25535-25551.

Zwally, H.J. and P. Gloersen, 1977: Passive microwave images of the polar region and research applications. *Polar Rec.*, 18, 431-450.

List of Acronyms

ADEOS- Advanced Earth Observing Satellite
AMSR - Advanced Microwave Scanning Radiometer
AMSU - Advanced Microwave Sounding Unit
DMSP - Defense Meteorological Satellite Program
EOS - Earth Observing System
ERS - European Remote Sensing Satellite
FNMOC - Fleet Numerical Meteorology and Oceanography Center
GHz - Gigahertz
GOES - Geosynchronous Operational Environmental Satellite
HPC - NCEP Hydrometeorological Prediction Center
IR - Infrared
LST - Local Standard Time
MPC - NCEP Marine Prediction Center
MW - Microwave
NCEP - NOAA/NWS National Centers for Environmental Prediction
NESDIS - NOAA National Environmental Satellite, Data, and Information Service
NOAA - National Oceanic and Atmospheric Administration
NPPU - National Precipitation Prediction Unit
NWS - NOAA National Weather Service
ORA - NESDIS Office of Research and Applications
RAMM - NESDIS Regional and Mesoscale Meteorology Division
RAMSDIS - NESDIS RAMM Advanced Meteorological Satellite Demonstration and Interpretation System
SAB - NESDIS Satellite Analysis Branch
SSM/I - Special Sensor Microwave Imager
TB - Brightness Temperature
TMI - TRMM Microwave Imager
TPW - Total Precipitable Water
TRMM - Tropical Rainfall Measuring Mission
VIS - Visible